Directed percolation: mean field theory and series expansions for some two-dimensional lattices

1983 J. Phys. A: Math. Gen. 16 385

(http://iopscience.iop.org/0305-4470/16/2/020)

J. Phys. A: Math. Gen. **16** (1983) 385–404. Printed in Great Britain

Directed percolation: mean field theory and series expansions for some two-dimensional lattices

K De'Bell†§ and J W Essam‡

† Department of Physics, University of Edinburgh, Edinburgh, Scotland
‡ Mathematics Department, Westfield College, University of London, Hampstead, London NW3 7ST, England

Received 12 July 1982

Abstract. The shape of percolation clusters in the directed percolation problem is studied within mean field theory.

Low-density series expansions are obtained for bond and site problems on the square and triangular lattices. These are used to test a scaling formula for the pair connectedness which involves two lengths $\xi_{\parallel}(\rho)$ and $\xi_{\perp}(\rho)$. Determination of the exponents $\nu_{\parallel}$ and $\nu_{\perp}$ for these lengths shows that all four problems are in the same universality class and the values support the hyperscaling relation

$$\beta = \tfrac{1}{2}(D\nu_{\perp} + \nu_{\parallel} - \gamma).$$

An independent argument is given for this relation.

1. Introduction

Recent interest in directed percolation theory (Broadbent and Hammersley 1957, Mauldon 1961) stems from its connection with a variety of physical problems: for example Reggeon field theory (Cardy and Sugar 1980), random resistor–diode networks (Redner and Brown 1981), chemical reactions (Schögl 1972, Grassberger and de la Torre 1979), epidemic models (Grassberger 1982) and galactic evolution (Schulman 1982).

The model is in a different universality class from isotropic percolation (Blease 1977a, b, c) and has two connectedness lengths $\xi_{\parallel}$ and $\xi_{\perp}$ (Kinzel and Yeomans 1981) parallel and perpendicular to the direction in which percolation first occurs.

The mean field theory of De'Bell and Essam (1981, hereafter DBE) is extended to directed problems in § 2 and the shape of the clusters is studied above and below ρ_c. The two connectedness lengths are found to have exponents $\nu_{\parallel} = 1$ and $\nu_{\perp} = \frac{1}{2}$. These results also follow from the work of Obukhov (1980), who showed that mean field exponents are valid above the critical dimension $d_c = 5$. Our results hold for any model whose direct connections satisfy (2.11). Essentially, the capture region of a given point should have a single symmetry axis and the probability of capture should be higher in one of the two axial directions. One could imagine more exotic systems with more than one axis and other symmetries, but here we consider only the simplest case in detail. Redner (1982a) has recently discussed a mean field theory for directed percolation which is based on the relation between percolation and models which

§ Permanent address: Department of Physics, Dalhousie University, Halifax, Nova Scotia, Canada B3H 3J5.

0305-4470/83/020385+20$02.25

have a Hamiltonian; the DBE theory is independent of such a connection. Harms and Strayley (1982) have also obtained the mean field values of $\nu_\parallel$ and $\nu_\perp$ by embedding a directed Cayley tree in an infinite-dimensional cubic lattice.

Cardy and Sugar (1980) have given the scaling form for the pair connectedness $C(\boldsymbol{x}, t)$ based on the equivalence with Reggeon field theory. Their relation is written in terms of the percolation functions $\xi_\parallel$, $\xi_\perp$ and the mean size S in equation (3.1). The prefactors are chosen so that integration of $C(\boldsymbol{x}, t)$ over the whole space correctly gives the mean size. However, integration along the special axis $\boldsymbol{x} = \boldsymbol{0}$ only, gives the expected number S_0 of particles per unit area on this axis which are connected to the origin. The scaling form (3.1) implies that S/S_0 diverges with exponent $D\nu_\perp$ (§ 3), where D is the number of transverse directions and we estimate this exponent directly as a test of the scaling form.

The argument of Dunn *et al* (1975a) which produces the hyperscaling relation $\beta = \frac{1}{2}(D\nu - \gamma)$ for isotropic percolation has no simple extension to the directed case. In § 3 we present a new argument which also yields the generalised relation $\beta = \frac{1}{2}(D\nu_\perp + \nu_\parallel - \gamma)$ for directed percolation (see also Cardy and Sugar (1980) and Redner (1982a)). This relation determines d_c in a simple way by insertion of the mean field exponents (Redner 1982a). Our numerical estimates of γ, $\nu_\perp$ and $\nu_\parallel$ in two dimensions are in excellent agreement with hyperscaling when compared with the series estimate of β (Blease 1977c). If hyperscaling is valid, then the scaling form (3.1) may be written

$$C(\boldsymbol{x}, t) \sim |\rho - \rho_c|^{2\beta} \Psi(|\rho - \rho_c|^{\nu_\perp} \boldsymbol{x}, |\rho - \rho_c|^{\nu_\parallel} t) \tag{1.1}$$

where β is the exponent for the vanishing of the percolation probability.

The remainder of the paper is concerned with the derivation (§ 4) and analysis (§ 5) of low-density series expansions for bond and site problems on the square and triangular lattices. The exponents resulting from this analysis are summarised in table 5. The main idea in § 4 is that two methods previously used by Blease (1977a, b) can be combined in a complementary manner to produce longer series.

2. A generalised percolation model and mean field theory

Consider the general model of DBE in which two types of particle, 'ordinary' and 'impurity', were distributed through a volume Ω with density $\rho(\boldsymbol{r})$ and $\nu(\boldsymbol{r})$ respectively. The model includes directed percolation theory as, for example, the case when the capture region $\omega(\boldsymbol{r})$ for a particle at $\boldsymbol{r}$ has a centre of mass which is not at $\boldsymbol{r}$. If for all $\boldsymbol{r}$ the centre of mass of $\omega(\boldsymbol{r})$ is displaced by $\boldsymbol{R}$ from $\boldsymbol{r}$, then, as ρ is increased, percolation will first occur in the direction of $\boldsymbol{R}$. Equations (3.1)–(3.6) of DBE, which give the percolation probability and mean size of clusters in the mean field approximation, are still valid for directed percolation. However, the subsequent equations of DBE § 3, which refer to the pair connectedness, break down when there is a preferred direction. In this section we extend the mean field theory to the angular dependence of the pair connectedness.

Before calculating the pair connectedness, we note that the model of DBE may be extended to include randomness in the particle connections as well as in the particle distribution. Replacement of (2.2)–(2.4) and (2.15) by the following definitions allows the results of DBE to be used for the generalised model.

Let $\gamma(\boldsymbol{r}, \boldsymbol{r}_0)$ be the (given) probability that a particle placed at $\boldsymbol{r}$ will be directly connected to a particle at $\boldsymbol{r}_0$. In DBE $\gamma(\boldsymbol{r}, \boldsymbol{r}_0)$ was equal to one for $\boldsymbol{r}$ in the capture

region of r_0 but zero otherwise. For a given configuration of the particles in which there are particles at r and r_0 let $\gamma_c(r, r_0)$ be the probability that there is a path from r_0 to r (i.e. a direct or indirect connection from r_0 to r).

The percolation probability may be defined by

$$P(r) = 1 - \langle E_c(r) \rangle_F \tag{2.1}$$

where the average over configurations of ordinary particles gives zero weight to configurations in which the cluster connected to a particle at r is of unbounded extent. As before,

$$E_c(r) = \exp\left(- \int \nu(r') \gamma_c(r', r)\, dr' \right) \tag{2.2}$$

is the probability that in a given configuration of ordinary particles the cluster at r will be free from impurity particles. Finally, the pair connectedness $C(r \mid r_0)$ and mean size $S(r)$ are defined by

$$C(r \mid r_0) = \langle \gamma_c(r, r_0) E_c(r_0) \rangle_F \tag{2.3}$$

and

$$S(r) = \frac{\langle \int \rho(r') \gamma_c(r', r) E_c(r)\, dr' \rangle_F}{n(r)(1 - P(r))} = \frac{1}{n(r)(1 - P(r))} \int \rho(r') C(r' \mid r)\, dr'. \tag{2.4}$$

The integral is the expected number of ordinary particles in the cluster at r giving zero weight to unbounded or impure clusters, and $n(r)$ is the expected number of ordinary particles directly connected to a particle at r:

$$n(r) = \int \rho(r') \gamma(r', r)\, dr'. \tag{2.5}$$

The definition of $S(r)$ agrees with that of DBE when ρ is constant, provided that we define $v(r)$ by

$$v(r) = \int \gamma(r', r)\, dr'. \tag{2.6}$$

In the case of directed percolation, we shall also be interested in the expected number of ordinary particles per unit perpendicular area which are connected to the origin and lie near the straight line through r, having direction of the unit vector e. With the same normalisation as $S(r)$, this is given by

$$S_e(r) = \frac{1}{n(r)(1 - P(r))} \int_{-\infty}^{\infty} \rho(r + se) C(r + se \mid r)\, ds. \tag{2.7}$$

The mean field equation for the pair connectedness is given by the generalisation of equation (2.14) of DBE, that is

$$C(r \mid r_0) = (1 - P(r_0)) \left(\gamma(r, r_0) + \int C(r \mid r') \rho(r') \gamma(r', r_0)\, dr' \right). \tag{2.8}$$

Assuming ρ to be constant and that $\gamma(r', r_0) = \gamma(r' - r_0)$, P will be constant and C will depend only on $r - r_0$. Taking Fourier transforms

$$\tilde{C}(k) = \frac{v(1 - P)}{\theta^{-1}(k) - n(1 - P)} \tag{2.9}$$

where

$$\gamma(\boldsymbol{r}) = \frac{v}{(2\pi)^d} \int e^{i\boldsymbol{k}\cdot\boldsymbol{r}} \theta(\boldsymbol{k})\, d\boldsymbol{k} \tag{2.10}$$

with $\theta(\boldsymbol{0}) = 1$. Now assume $\theta(\boldsymbol{k})$ to be of the form

$$\theta(\boldsymbol{k}) = \frac{b^2 - a^2}{b^2 - a^2 + (k^2 + 2i\boldsymbol{k}\cdot\boldsymbol{a})\phi(\boldsymbol{k})} \qquad b > a > 0 \tag{2.11}$$

where $\phi(\boldsymbol{k}) \sim 1 + O(k^2)$ for $k \to 0$ and $\phi(\boldsymbol{k}) \to \infty$ sufficiently fast to ensure the convergence of subsequent integrals as $k \to \infty$. We take this to be the simplest form of $\theta(\boldsymbol{k})$ having the required symmetry for directed percolation. (However, it may readily be shown that if, for example, the capture region for point $\boldsymbol{r}$ is an orientated d-dimensional cube of side 1 with centre displaced by $\boldsymbol{a}$ from $\boldsymbol{r}$ parallel to some face of the cube, then $\theta(\boldsymbol{k})$ may be approximated by (2.11) for small $|\boldsymbol{k}|$ and $|\boldsymbol{a}| \ll \frac{1}{2}$.) Assuming (2.11), then for $r \to \infty$

$$\gamma(\boldsymbol{r}) \sim e^{-(br + \boldsymbol{a}\cdot\boldsymbol{r})} / r^{(d-1)/2} \tag{2.12}$$

which decays exponentially in all directions but the decay rate is least in the direction of $\boldsymbol{a}$. For this model

$$\tilde{C}(\boldsymbol{k}) = \frac{v(1-P)(b^2 - a^2)}{\kappa^2 - a^2 + (k^2 + 2i\boldsymbol{k}\cdot\boldsymbol{a})\phi(\boldsymbol{k})} \tag{2.13}$$

and for fixed n and $r \to \infty$

$$C(\boldsymbol{r}) \sim e^{-(\kappa r - \boldsymbol{a}\cdot\boldsymbol{r})} / r^{(d-1)/2} \tag{2.14}$$

where

$$\kappa^2 = a^2 + (b^2 - a^2)(1 - n + nP). \tag{2.15}$$

The shape of a typical cluster is determined primarily by the exponent $\kappa r - \boldsymbol{a}\cdot\boldsymbol{r}$, and curves along which this has value 1 are plotted for $a = 1$ and various values of κ in figure 1.

Now $P = 0$ for $n < 1$ and $\rho \simeq 2(n-1)$ for $n \to 1^+$ (DBE 3.2). Hence from (2.14) we see that, as $n \to n_c = 1$ from either side, $\kappa \to a$ and the decay length becomes infinite in the direction of $\boldsymbol{a}$ but is still finite in any other direction. Near n_c

$$\kappa^2 - a^2 \simeq 2a(\kappa - a) \simeq (b^2 - a^2)|n - 1| \tag{2.16}$$

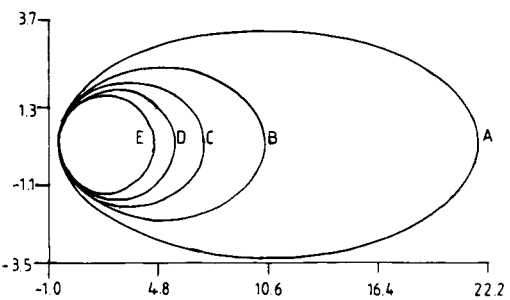

Figure 1. Curves of unit decay length in the mean field approximation for various values of κ^2: A, $\kappa^2 = 1{,}1$; B, 1.2; CC, 1.3; D, 1.4; E, 1.5.

so that the finite clusters at $n > n_c$ are similar to those for $n < n_c$ at the same distance from n_c. If we define $\xi_\parallel$ to be the decay length in the forward direction and $\xi_\perp$ to be the maximum value of x for the curves in figure 1 then it can be shown that

$$\xi_\parallel = (\kappa - a)^{-1} \simeq \frac{2a}{b^2 - a^2}|n-1|^{-1} \tag{2.17}$$

and

$$\xi_\perp \simeq (\kappa^2 - a^2)^{-1/2} \simeq (b^2 - a^2)^{-1/2}|n-1|^{-1/2}. \tag{2.18}$$

For fixed $n \neq n_c$ and typical points in a large cluster ($x \ll t$) the pair connectedness may be approximated by the form

$$C(\boldsymbol{r}) \sim \frac{e^{-t/\xi_\parallel} e^{-[(x/\xi_\perp)^2/4]/(t/\xi_\parallel)}}{r^{(d-1)/2}} \tag{2.19}$$

and for $k \to 0$

$$\tilde{C}(k) \simeq S[1 - ik_\parallel\xi_\parallel - (k_\parallel\xi_\parallel)^2 - (k_\perp\xi_\perp)^2 + \ldots]. \tag{2.20}$$

The asymptotic form of the moments of $C(\boldsymbol{r})$ is therefore given by

$$\mu_{1t} \simeq S\xi_\parallel \qquad \mu_{2t} \simeq 2S\xi_\parallel^2 \qquad \mu_{2x} \simeq 2S\xi_\perp^2. \tag{2.21}$$

The directional mean size in the preferred direction defined by (2.7) with $\boldsymbol{e} = \boldsymbol{a}/a$ is given by

$$S_0 = \frac{1}{v(1-P)} \frac{1}{(2\pi)^D} \int d\boldsymbol{k}_\perp \tilde{C}(\boldsymbol{k}_\perp, k_\parallel = 0). \tag{2.22}$$

The integral is proportional to the generating function for random walks in $D = d-1$ dimensions which return to the origin.

$$S_0 = \frac{b^2 - a^2}{(2\pi)^D} \int d\boldsymbol{k}_\perp \frac{1}{\kappa^2 - a^2 + \phi(\boldsymbol{k}_\perp)k_\perp^2} \tag{2.23}$$

$$\sim (\kappa^2 - a^2)^{D/2-1} \sim |n-1|^{-\gamma_0} \tag{2.24}$$

where $\gamma_0 = 1 - D/2$ and for $D > 2$ the expression refers to the singular part of S_0. When $D = 2$, S_0 diverges logarithmically.

So far we have considered only the pair connectedness between points given that the connecting path belongs to a cluster which is finite in the preferred direction. For $n > n_c$ the clusters which are of infinite extent in the preferred direction are still finite in direction whose angular deviation from the preferred direction is $\phi > \phi_c(n)$. To see this we must drop the factor $1-P$ in (2.8), which means setting $P = 0$ in (2.9). For $n > n_c = 1$, we now have $\kappa < a$ and ϕ_c is obtained by setting the exponent to zero in (2.15); thus

$$\cos\phi_c(n) = \kappa/a. \tag{2.25}$$

We show in figure 2 the curves along which the exponent $\kappa r - \boldsymbol{a}\cdot\boldsymbol{r}$ has the value α for a range of α with $a = 1$ and $\kappa^2 = 0.9$. The curves are asymptotically parallel to the $\alpha = 0$ line, which is at an angle $\phi_c = \tan^{-1}(\frac{1}{3})$. For $n \to n_c^+$

$$\phi_c \simeq \frac{(b^2 - a^2)^{1/2}}{a}(n-1)^{1/2} \simeq \frac{2\xi_\perp}{\xi_\parallel} \tag{2.26}$$

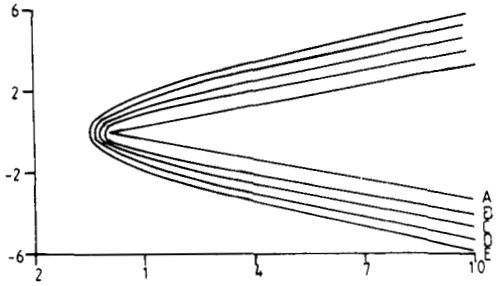

Figure 2. The curves $\kappa r - \boldsymbol{a} \cdot \boldsymbol{r} = \alpha$ for $a = 1$ and $\kappa^2 = 0.9$ for various values of α: A, $\alpha = 0.0$; B, 0.25; C, 0.5; D, 0.75; E, 1.0.

in agreement with the general result of Harms and Strayley (1982) which was based on the superlattice picture of the infinite cluster (Skal and Shklovskii 1975) and confirmed for a Cayley tree model.

3. Scaling and hyperscaling

Cardy and Sugar (1980) have established an equivalence between directed percolation and Reggeon field theory which enabled them to take over a scaling relation which was obtained for the field theory by Abarbanel *et al* (1976). The relation may be written in the form

$$C(\boldsymbol{x}, t) \simeq vS\xi_\perp^{-D}\xi_\parallel^{-1}\phi(\boldsymbol{x}/\xi_\perp, t/\xi_\parallel) \tag{3.1}$$

where v is the constant 'volume' of the capture region and the factors S, $\xi_\perp$ and $\xi_\parallel$ are functions of the assumed uniform density ρ and are singular at ρ_c:

$$S \sim |\rho - \rho_c|^{-\gamma}, \xi_{\perp,\parallel} \sim |\rho - \rho_c|^{-\nu_{\perp,\parallel}}. \tag{3.2}$$

The prefactors are chosen for consistency with the mean size S being related to the integral of C by (2.4).

The series expansions in the next section will be used to test this relation by estimating $\nu_\perp$ in two different ways. Firstly we use

$$\frac{\mu_{2x}}{S} = \int \mathrm{d}^D x \, \mathrm{d}t \, x^2 \frac{C(\boldsymbol{x}, t)}{S} \sim \xi_\perp^2 \sim |\rho - \rho_c|^{-2\nu_\perp} \tag{3.3}$$

and secondly the mean size in the preferred direction, which, from (2.7), is

$$\frac{S_0}{S} \simeq \xi_\perp^{-D}\xi_\parallel^{-1} \int \mathrm{d}t \, \phi(\boldsymbol{0}, t/\xi_\parallel) \sim \xi_\perp^{-D} \sim |\rho - \rho_c|^{D\nu_\perp}. \tag{3.4}$$

This formula implies the exponent relation

$$\gamma_0 = \gamma - D\nu_\perp \tag{3.5}$$

where γ_0 describes the divergence of S_0. This relation is satisfied for all D by the mean field exponents (equation (2.24)).

Another field theory relation which was exhibited by Cardy and Sugar (1980) is for the percolation probability exponent and may be written

$$\beta = \tfrac{1}{2}(D\nu_\perp + \nu_\parallel - \gamma). \tag{3.6}$$

The series expansions of the next section will determine all three exponents on the right of the equation, and the relation will be tested by comparison with independent estimates of β. Equation (3.6) is a hyperscaling relation and is satisfied only by mean field exponents at $D = D_c = 4$, which gives $d_c = 5$. Obukhov (1980) has shown that the mean field exponents are valid above this critical dimension, and (3.6) is only expected to be valid for $d \leqslant 5$.

Dunn *et al* (1975a) obtained the above relation in the undirected case ($\nu_\perp = \nu_\parallel$) using only percolation concepts and in particular the mean number of clusters. The latter does not extend easily to directed percolation, since clusters are only defined relative to a given source, and sources which are not in each other's cluster may still have particles in common.

We now obtain (3.6) for ordinary percolation by an argument which avoids the mean number of clusters and extends immediately to the directed problem. Consider the superlattice picture of the infinite cluster discussed by Skal and Shklovskii (1975) and used by Harms and Strayley (1982) and Redner (1982b) in the context of directed percolation. This is an irregular lattice-like structure with nodes separated by a distance of the order of the connectedness length $\xi(\rho)$. Coexisting with the infinite cluster are finite clusters of a similar linear dimension $\xi(\rho)$, and size distribution which is scaled by a parameter $\mathscr{S}(\rho) \sim |\rho - \rho_c|^{-\Delta}$. If we suppose that the nodes of the superlattice contain of order $\mathscr{S}(\rho)$ particles so that they have a size comparable with typical finite clusters in the neighbourhood, then the probability that a particle belongs to an infinite cluster $P(\rho)$ is estimated by

$$P(\rho) \sim \mathscr{S}(\rho)/(\xi(\rho))^d \sim |\rho - \rho_c|^{d\nu - \Delta} \tag{3.7}$$

so that

$$\beta = d\nu - \Delta. \tag{3.8}$$

This result is obtained by counting the number of particles per unit volume which belong to the infinite cluster. Recalling the scaling formula (Dunn *et al* 1975a)

$$P(\rho, h) \sim P(\rho) f(h\mathscr{S}(\rho)) \tag{3.9}$$

where the impurity density $\nu(\boldsymbol{r})$ is assumed constant and $h = \nu(\boldsymbol{r})v$, then, since $S(\rho) \propto \partial P/\partial h$,

$$\Delta = \beta + \gamma. \tag{3.10}$$

Combining this with (3.8) gives

$$\beta = \tfrac{1}{2}(\mathrm{d}\nu - \gamma). \tag{3.11}$$

The extension to directed percolation is now clear. Noting that the superlattice cells will have dimension of order $\xi_\parallel$ in the preferred direction and $\xi_\perp$ in the D perpendicular directions, we obtain

$$P(\rho) \sim \mathscr{S}(\rho)/(\xi_\parallel(\rho)\xi_\perp^D(\rho)) \tag{3.12}$$

and

$$\beta = D\nu_\perp + \nu_\parallel - \Delta. \tag{3.13}$$

Since (3.10) is still valid, the result (3.6) follows.

4. Low-density series expansions for two-dimensional lattice models

The basic method used has been described in detail by Blease (1977a), who derived series expansions for the mean size and second spherical moment of various two-dimensional bond problems. The method is limited by the amount of computer memory available, and here we show how the data may be considerably extended without using further storage space. Both bond and site problems have been considered on the directed square and triangular lattices studied by Blease (1977a, figures 1(*a*) and (*b*)).

The extension is based on classifying the lattice sites according to the least number of steps σ required to reach a site from a given origin (observing the direction of the bonds). Let N_σ be the set of sites which are σ steps away. We shall use the variable p which is the probability of an open bond or the probability of an occupied site. To make a connection with the particle description of the previous sections, write $p = 1-e^{-p}$, which is the probability that a site (or bond) is occupied by at least one particle (Coniglio and Essam 1977). Integrals over Ω are replaced by sums over lattice sites. Thus the moments of the pair connectedness may be written

$$\mu_{lm}(p) = \sum_{\sigma=0}^{\infty} \sum_{i \in N_\sigma} x_i^l t_i^m C_i(p) \tag{4.1}$$

where x_i and t_i are the coordinates of site i relative to axes perpendicular to and along the preferred direction (i.e. the (1, 1) direction for the lattices considered). We consider only the mean size $S(p) = p_F^{-1}\mu_{00}(p)$ and the second moments $\mu_2^{(x)}(p) = \mu_{20}(p)$ and $\mu_2^{(t)} = \mu_{02}(p)$. $\mu_{11}(p) = 0$ by symmetry. (For $p < p_c$, $p_F = 1$ for the bond problem and $p_F = p$ for the site problem.) To obtain low-density series expansions through order N, only terms with $\sigma \leqslant N$ need be calculated. The method described by Blease (1977a), which is essentially a transfer matrix method, has been used for $\sigma \leqslant N_1$, where N_1 is as large as possible consistent with the computer memory available. For $N_1 < \sigma \leqslant N$, we have used a weak sub-graph expansion (Dunn *et al* 1977b). The application of this method to directed lattices has been described by Blease (1977b) in the case of the mean size, and here we extend his description to the second moments.

In principle, the method works on any lattice, but the implementation is most straightforward on the square, hypercubic and body-centred cubic lattices. From here on we restrict the discussion to these lattices. The directed sub-graphs which have non-zero weight are unions of directed paths between the two 'root' vertices (Essam 1980) and, in calculating $C_i(p)$, one root is mapped to the origin and the second to site i. All paths between the roots must be of the same length and for a given site $i \in N_\sigma$ the paths must all have σ steps. Also the coordinate t_i is proportional to σ. The triangular lattice has neither of these properties: for this lattice we have used only the transfer matrix method for the bond problem, and the perimeter method (Domb 1959) together with an animal-counting program for the site problem.

Before calculating the sub-graph weights we must consider the construction of a list of graphs required for $N_1 < \sigma \leqslant N$. We note that, for $i \in N_\sigma$, $C_i(p)$ is a polynomial in p, the lowest power of p being σ. Also, a graph with r edges ($r+1$ vertices) contributes only to the coefficient of p^r for the bond (site) problem, thus $\sigma \leqslant r \leqslant N$. Now the shortest path through a required graph must be of length σ, hence, for $r = \sigma$, only chains of r edges need be considered. For the bond problem this is also true when $r = \sigma + 1$, but for the site problem a chain with an embedded square must also

be considered (figure 4(*a*) of Blease (1977b)). This graph enters at $r = \sigma + 2$ for the bond problem. In general, if $r = \sigma + u$, the graphs to be considered have as many as u edges (vertices) which may be deleted without disconnecting the roots. The graphs required for the bond and site problems on the hypercubic lattices are listed in table 1 for different values of u. The letters refer to figure 4(*a*) of Blease (1977b) except for the graph

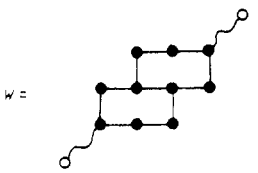

which is missing from his list.

Table 1. Graphs which enter the expansion when the number of edges $r = \sigma + u$. The letters refer to figure 4(*a*) of Blease (1977b).

u	Bond problem	Site problem
1		(*a*)
2	(*a*)	(*b*)–(*d*)
3	(*b*)	(*e*)–(*g*), (*i*), (*j*), (*l*), (*o*), (*s*), (*v*)
4	(*c*)–(*e*)	
5	(*f*)–(*i*)	
6	(*j*)–(*w*)	

To obtain the contribution of the graphs in table 1 to the mean size it is only necessary to count the total number of embeddings on the lattice and weight this with $(-1)^{j-1}$, where j is the number of independent paths which constitute the graph (Arrowsmith and Essam 1977). Formulae for the number of embeddings were given by Blease (1977b, table 4).

In calculating the second moments, an additional factor must be included. For the case of $\mu_2^{(r)}$ this is just σ^2. The weight for $\mu_2^{(x)}$ is not so simple and depends on the lattice and structure of the graph. For the linear chain it is the mean square end-to-end distance for a random walk on the D-dimensional lattice obtained by projecting the d-dimensional lattice onto a plane perpendicular to the t axis. This is proportional to the number of steps r. The general graph which contributes to the expansion of the pair connectedness is a chain of non-nodal one-irreducible, two-rooted graphs. Each of these graphs must also have the property that all paths between the roots have the same number of steps. We now consider the weight to be used in calculating $\mu_2^{(x)}$.

Suppose that $G_1, \ldots, G_M$ is a collection of two-rooted, non-nodal graphs of the above type, each with a distinguished initial and terminal root. Let G be the two-rooted graph obtained by attaching the initial vertex of G_{i+1} to the terminal vertex of G_i, $i = 1, \ldots, M-1$, and let $\boldsymbol{R}_i = (\boldsymbol{x}_i, t_i)$ be the position vector of the terminal root of G_i relative to its initial vertex in a given embedding of G on the lattice. The contribution

of G to $\mu_2^{(x)}$ is $(-1)^{j-1}p^r W_2^{(x)}(G)$ where

$$W_2^{(x)}(G) = \sum_{\boldsymbol{R}_1} \ldots \sum_{\boldsymbol{R}_M} (\boldsymbol{x}_1 + \ldots + \boldsymbol{x}_M)^2 \prod_{i=1}^{M} W_i(\boldsymbol{R}_i). \tag{4.2}$$

Here $W_i(\boldsymbol{R}_i)$ is the number of embeddings of G_i with its initial and terminal roots at relative positions $\boldsymbol{R}_i$. The product is the number of embeddings of G with its roots and nodal points in fixed positions, which factorises since vertices in different G_i may be embedded independently. The sum may be rearranged as

$$W_2^{(x)}(G) = W(G) \sum_{j=1}^{M} \sum_{k=1}^{M} \langle \boldsymbol{x}_j \cdot \boldsymbol{x}_k \rangle \tag{4.3}$$

where $W(G)$ is the total number of embeddings of G and $\langle\ \rangle$ represents the average over embeddings. Then

$$W(G) = \prod_{i=1}^{M} W(G_i) \tag{4.4}$$

with

$$W(G_i) = \sum_{\boldsymbol{R}_i} W_i(\boldsymbol{R}_i). \tag{4.5}$$

For $j \neq k$ the average may be written as $\langle \boldsymbol{x}_j \rangle \cdot \langle \boldsymbol{x}_k \rangle$ where

$$\langle \boldsymbol{x}_i \rangle = \frac{1}{W(G_i)} \sum_{\boldsymbol{r}_i} W_i(\boldsymbol{r}_i)\boldsymbol{x}_i. \tag{4.6}$$

On the lattices considered, $\langle \boldsymbol{x}_i \rangle = \boldsymbol{0}$ and hence

$$W_2^{(x)}(G) = W(G) \sum_{i=1}^{M} \langle x_i^2 \rangle. \tag{4.7}$$

The $W(G)$ are essentially given by the formulae of Blease (1977b, table 3), except that he has collected together all possible orderings and directing of the G_i. In table 2 we list the factor $\sum_{i=1}^{M} \langle x_i^2 \rangle$ for the square lattice in units of $\langle x_1^2 \rangle$ for a single edge. For a chain of r single edges the sum is equal to r in these units.

The contribution of G to the directed mean size $S_0(p)$ in the preferred direction is obtained by replacing $W(G)$ by $W_0(G)$, the number of embeddings in which the second root is at a point on the t axis. This may be written

$$W_0(G) = \sum_{\boldsymbol{R}_1} \ldots \sum_{\boldsymbol{R}_{M'}} \rho_{r-r'}(-\boldsymbol{x}_1 - \boldsymbol{x}_2 - \ldots - \boldsymbol{x}_{M'}) \prod_{i=1}^{M'} W_i(\boldsymbol{R}_i) \tag{4.8}$$

where the vectors $\boldsymbol{R}_1, \ldots, \boldsymbol{R}_{M'}$ are the ones corresponding to the G_i having more than one edge, r' is the total number of edges in these G_i, and $\rho_n(\boldsymbol{x})$ is the number of n-step random walks on the D-dimensional projected lattice which end at the point $\boldsymbol{x}$ ($\rho_0(\boldsymbol{0}) = 1$). For the square lattice these are walks on a linear chain, and for $|x| \leq n$

$$\rho_n(x) = \begin{cases} \binom{n}{\frac{1}{2}(n-x)} & n-x \text{ even} \\ 0 & n-x \text{ odd.} \end{cases} \tag{4.9}$$

The factors $\prod_{i=1}^{M'} w_i(\boldsymbol{R}_i)$ are given in table 2 for the square lattice.

Table 2. Weights for calculating $\mu_2^{(x)}(p)$ and $S_0(p)$ for bond and site problems on the square lattice. r is the number of edges; $x = x_1 + x_2 + \ldots + x_{M'}$.

Graph	$\sum_{i=1}^{M} \langle x_i^2 \rangle$	$\prod_{i=1}^{M'} w_i(\boldsymbol{R}_i)$ for $x \geqslant 0$				
		$x=0$	1	2	3	4
(*a*)	$r-4$	1				
(*b*)	$r-5$		1			
(*c*)	$r-6$		1			
(*d*)	$r-8$	1				
(*e*)	$r-32/5$	3		1		
(*g*)	$r-7$	2		1		
(*h*)	$r-55/7$		6		1	
(*i*)	$r-9$		1			
(*l*)	$r-6$			1		
(*m*)	$r-10$	2				
(*o*)	$r-10$	2				
(*p*)	$r-10$	2				
(*q*)	$r-42/5$		4		1	
(*r*)	$r-28/3$	20		10		1
(*s*)	$r-12$	1				
(*t*)	$r-10$	2		1		
(*u*)	$r-52/5$	3		1		
(*v*)	$r-10$		1			
(*w*)	$r-8$		3		1	

5. Series analysis

The low-density series we have used are tabulated in the Appendix. Some of the series for the bond problem have been published previously (Blease 1976, 1977a, Essam and De'Bell 1981) but we include them for completeness.

5.1. Critical probability and mean size exponent

All our exponent estimates are based on standard Padé pole–residue analysis of the Dlog series. The Padé tables for the mean size series are shown in table 3. As usual in this type of analysis there is a strong correlation between estimates of the critical points and exponents. The scatter of p_c estimates is least in the case of the square lattice bond problem. Blease (1977a) found that more consistent estimates of p_c for this problem could be obtained by applying the ratio method to the Euler-transformed series with $p = z/(1-z)$. Our four extra terms enable us to extend his table 2(*a*) and the results are shown in table 4. The estimates of z_c remain remarkably steady and we confirm his rather conservative result

$$p_c(\text{square bond}) = 0.6446 \pm 0.0002.$$

This is also in good agreement with the finite size scaling values of Kinzel and Yeomans (1981).

Table 3. Poles and residues of the Dlog mean size series.

(*a*) Square lattice, bond problem

	$N/N-2$		$N/N-1$		N/N		$N/N+1$		$N/N+2$	
N	p_c	γ	p_c	γ	p_c	γ	p_c	γ	p_c	γ
8	0.6455	2.321	0.6452	2.306	0.6444	2.259	0.6453	2.313	0.6476	2.423
9	0.6462†	2.340	0.6447	2.282	*	*	0.6454†	2.319	0.6447	2.275
10	0.6451	2.299	0.6448	2.289	0.64482†	2.285	0.64473	2.279	0.64472	2.279
11	0.64477†	2.282	*	*	0.64472	2.279	0.64473†	2.279	0.64469	2.277
12	0.64466	2.274	0.64469	2.276	0.64461	2.269				
13	0.64467	2.275								

(*b*) Square lattice, site problem

N	p_c	γ	p_c	γ	p_c	γ	p_c	γ	p_c	γ
8	0.7006	2.072	*	*	0.6991^+	2.038^+	0.7098^+	2.607^+	0.7074	2.401
9	—	—	0.7023	2.121	0.7066^+	2.345^+	*	*	0.7065^+	2.333^+
10	0.7041	2.195	*	*	0.7057^+	2.279^+	0.7051^+	2.243^+	0.7036^+	2.146^+
11	*	*	0.7053^+	2.257^+	*	*	0.7049^+	2.232^+		
12	0.7050^+	2.238^+	0.7052^+	2.248^+						

(c) Triangular lattice, bond problem

N	p_c	γ	p_c	γ	p_c	γ	p_c	γ	p_c	γ
3	0.4839	5.098	0.4789	2.350	0.4813	2.414	0.4823	2.446	0.4780	2.283
4	0.4807	2.395	0.4831	2.480	0.4815†	2.420	0.4781	2.287	0.4780†	2.284
5	0.4810	2.404	0.4805	2.387	0.4778	2.271	0.4780	2.283	0.4780†	2.284
6	*	*	0.4784	2.300	0.4782	2.292	0.4781	2.288		
7	0.4781	2.288	0.4782	2.293						

(d) Triangular lattice, site problem

N	p_c	γ	p_c	γ	p_c	γ	p_c	γ	p_c	γ
3	0.6071	3.805	0.5666	1.695	0.6001	2.613	—	—	—	—
4	0.5753	1.825	—	—	—	—	0.5847	1.941	0.5995	2.467
5	0.5923	2.177	0.5932	2.203	0.5964	2.322	0.5969	2.347		
6	0.5920†	2.169	0.5970	2.352						

† defect; * interfering pole-zero pair; — no positive real root.

Table 4. Ratio method applied to the mean size series for the square lattice with $p = z/(1-z)$ and an n-shift of 4.16.

n	z_c	γ	n	z_c	γ
10	0.392 001	2.2711	18	0.391 951	2.2690
11	0.391 955	2.2692	19	0.391 952	2.2690
12	0.391 960	2.2694	20	0.391 951	2.2689
13	0.391 963	2.2696	21	0.391 954	2.2691
14	0.391 958	2.2693	22	0.391 954	2.2691
15	0.391 954	2.2691	23	0.391 949	2.2688
16	0.391 955	2.2692	24	0.391 957	2.2694
17	0.391 955	2.2692	25	0.391 952	2.2690

If p_c is given the value 0.6446, the pole–residue plot of the Padé data yields the biased estimate

$$\gamma(\text{square bond}) = 2.269 \pm 0.002 + 80\Delta p_c$$

which is also consistent with table 4. The remaining Padé tables are consistent with exponent universality, and using $\gamma = 2.269$ we obtain the biased estimates of the other critical points:

$$p_c(\text{square site}) = 0.7055 \pm 0.0001 + 0.02\Delta\gamma$$

$$p_c(\text{triangular bond}) = 0.4777 \pm 0.0001 + 0.02\Delta\gamma$$

$$p_c(\text{triangular site}) = 0.5949 \pm 0.0004 + 0.025\Delta\gamma.$$

5.2. Parallel connectedness length

The values of p_c given in (§ 5.1) have been used to estimate $\nu_\parallel$ from the pole–residue plots. Two series were used for each problem: $\mu_2^{(t)}(p)/S(p)$ and $\mu_2^{(r)}(p)/S(p)$, where $\mu_2^{(r)} = \mu_2^{(t)} + \mu_2^{(x)}$ is the second spherical moment previously analysed by Blease (1977a) for the bond problem. Since $\mu_2^{(x)}$ diverges less strongly than $\mu_2^{(t)}$, both functions are expected to have critical exponent $2\nu_\parallel$. If both sets of data are superimposed on a pole–residue plot, a single well defined curve is found for both square lattice problems. As an example we show the pole–residue plot for the square lattice site problem in figure 3. For the triangular lattice the curves run roughly parallel with a vertical separation of 0.01 in the region of the biased p_c estimates, and for the site problem the majority of estimates lie below this region. The results are summarised in table 5. The value

$$\nu_\parallel(\text{square bond}) = 1.730 \pm 0.005 + 50\Delta p_c$$

is our best estimate of $\nu_\parallel$, and bearing in mind that the quoted errors are only a measure of the scatter on the pole–residue plots, the somewhat lower values obtained from the other series are not inconsistent with this result. In the case of the bond problems our analysis is an extension of that of Blease (1977a) and our findings are not significantly different. Similar values have also been obtained by Kinzel and Yeomans (1981).

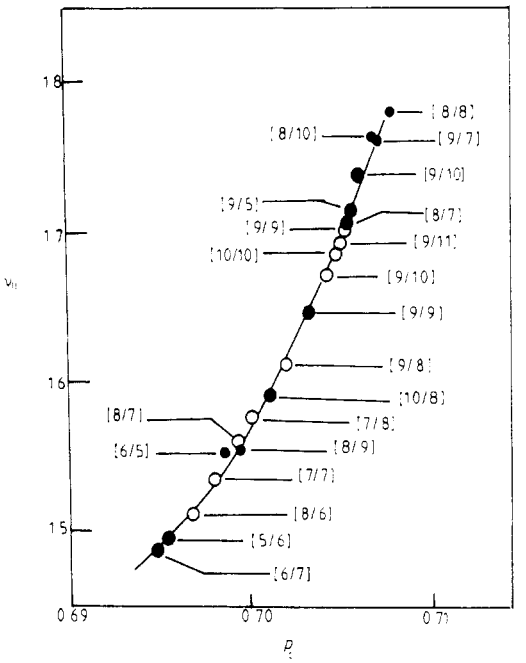

Figure 3. Pole-residue plots for $\nu_{\|}$ from $\mu_2^{(r)}/S$ (○) and $\mu_2^{(r')}/S$ (●): directed site problem, square lattice.

Table 5. Summary of critical probabilities and exponents for the square and triangular lattices.

	Square		Triangular	
	Bond	Site	Bond	Site
p_c	0.6446 ± 0.0002	$0.7055 + 0.0001 + 0.02\Delta\gamma$	$0.4777 \pm 0.0001 + 0.02\Delta\gamma$	$0.5949 + 0.0004 + 0.025\Delta\gamma$
γ	$2.269 \pm 0.002 + 80\Delta p_c$	2.269 (assumed)	2.269 (assumed)	2.269 (assumed)
$\nu_{\|}$	$1.730 \pm 0.005 + 50\Delta p_c$	$1.715 \pm 0.01 + 25\Delta p_c$	$1.71 \pm 0.02 + 25\Delta p_c$	$1.70 \pm 0.01 + 35\Delta p_c$
$\nu_{\perp}$	$1.095 \pm 0.002 + 30\Delta p_c$	$1.095 \pm 0.002 + 25\Delta p_c$	$1.095 \pm 0.005 + 20\Delta p_c$	$1.084 \pm 0.005 + 20\Delta p_c$
ν_0	$1.088 \pm 0.002 + 25\Delta p_c$	$1.095 \pm 0.005 + 15\Delta p_c$	$1.074 \pm 0.005 + 20\Delta p_c$	$1.094 \pm 0.01 + 10\Delta p_c$

5.3. Perpendicular connectedness length

In § 3 we saw that if the scaling form (3.1) is valid, the ratio $S(p)/S_0(p)$ should diverge with index $D\nu_{\perp}$. To test this result we let

$$S(p)/S_0(p) \sim (p_c - p)^{-D\nu_0}$$

and test the scaling law by comparing ν_0 with the value of $\nu_{\perp}$ obtained from the

expansion of $\mu_2^{(x)}(p)/S(p)$ which diverges with index $2\nu_\perp$. The pole–residue plots for all four problems are shown in figure 4, and exponent estimates are given in table 4.

The values of $\nu_\perp$ are in excellent agreement except for the triangular site problem. In this case the result depends heavily on the [6/4] approximant which gives a rather low value and should not be taken too seriously.

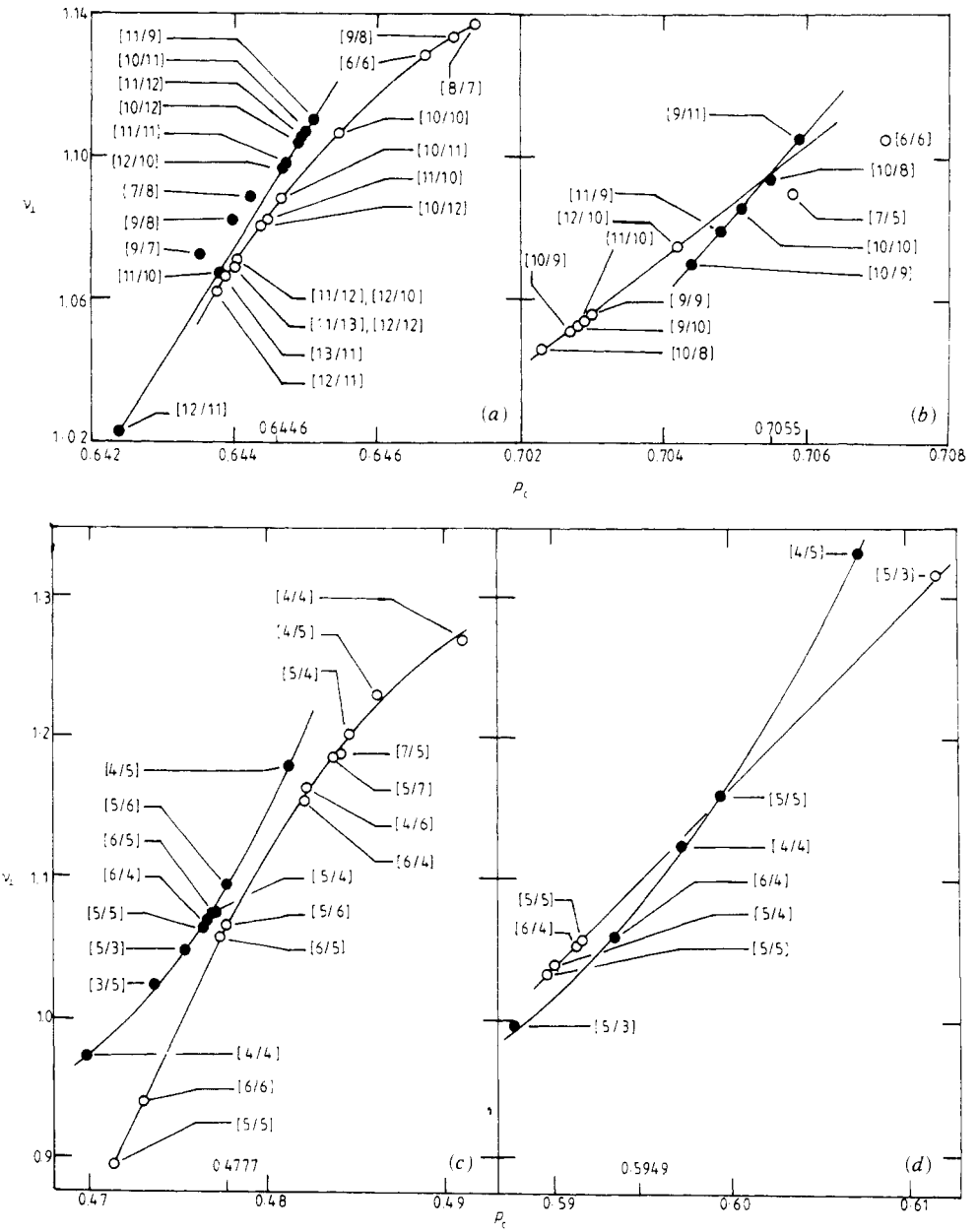

Figure 4. Pole–residue plots for $\nu_\perp$ from $\mu_2^{(x)}/S$ (●) and S/S_0 (○): (*a*) square lattice, bond problem; (*b*) square lattice, site problem; (*c*) triangular lattice, bond problem; (*d*) triangular lattice, site problem.

The bond problem curves for ν_0 are well defined but run parallel to those for $\nu_\perp$ in the assumed critical region rather than intersecting as we had hoped. This does not necessarily mean that the two exponents are different, since a similar effect was noticed in § 5.2 where the exponents were known to be the same. Similar effects have also appeared in other Padé analyses of percolation series (see e.g. Blease *et al* 1978). The discrepancy of 0.02 in the worst case is relatively small.

In the case of the site problem the estimates of ν_0 are in good agreement with those of $\nu_\perp$, although the assignment of errors is difficult since most of the points lie below the biased estimates of p_c.

6. Summary and discussion

It is clear from our results that all four models lie in the same universality class. The relatively small discrepancy between $\nu_\perp$ and ν_0 is not unprecedented and does not represent a significant violation of the scaling law (3.1).

Our results enable the right-hand side of (3.6) to be evaluated, and comparison with the result $\beta = 0.28 \pm 0.02$ (Blease 1977c) will be a test of hyperscaling. For the square lattice bond problem

$$\tfrac{1}{2}(D\nu_\perp + \nu_\parallel - \gamma) = 0.278 \pm 0.005$$

confirming (3.6). Notice that the systematic errors arising from Δp_c cancel, and the contribution from the variation with p_c is less than $5\Delta p_c$. For the other problems considered the results are consistent with (3.6) but less precise.

Lastly, we note that there is a slight discrepancy between the p^{11} term of the mean size and second spherical moment series presented here for the triangular lattice bond problem, and the results of Blease (1977a). In an attempt to check for word length and memory size errors, we have run our program on the University CDC 7600 as well as on the Prime 750 College computer on which most of the work was carried out; however, the discrepancy remains. In adding three more terms we have been able to apply some consistency checks to the p^{11} coefficient.

Appendix. Low-density series expansions for the directed square and triangular lattices

Tabulated below are the coefficients of p^m in the low-density series analysed in § 5.

(*a*) The square lattice bond problem (nearest-neighbour spacing $a = 1$).

m	$S(p)$	$S_0(p)$	$\mu_2^{(x)}(p)$	$\mu_2^{(t)}(p)$	$\mu_2^{(r)}(p)$
0	1	1	0	0	0
1	2	0	1	1	2
2	4	2	4	8	12
3	8	0	12	36	48
4	15	5	32	126	158
5	28	0	78	382	460
6	50	14	179	1047	1226

Table (*a*)—*continued*

m	$S(p)$	$S_0(p)$	$\mu_2^{(x)}(p)$	$\mu_2^{(t)}(p)$	$\mu_2^{(r)}(p)$
7	90	−4	393	2681	3074
8	156	42	832	6484	7316
9	274	−20	1717	15069	16786
10	466	126	3451	33723	37174
11	804	−100	6828	73524	80352
12	1348	400	13232	155970	169202
13	2300	−376	25386	324930	350316
14	3804	1248	47877	662617	710494
15	6450	−1556	89721	1334065	1423786
16	10547	4231	165647	2639033	2804680
17	17784	−5588	304748	5173100	5477848
18	28826	13880	553053	9988505	10541558
19	48464	−21912	1002426	19164778	20167204
20	77689	48985	1793437	36273493	38066930
21	130868	−76404	3211514	68392722	71604236
22	207308	165712	5675637	127298209	132973846
23	350014	−295660	10063269	236546749	246610018
24	548271	602237	17595595	434030369	451625964
25	931584	−1017452	30941598	796758862	827700460

(*b*) The square lattice site problem ($a = 1$)

m	$S(p)$	$S_0(p)$	$\mu_2^{(x)}(p)$	$\mu_2^{(t)}(p)$	$\mu_2^{(r)}(p)$
0	1	1	0	0	0
1	2	0	1	1	2
2	4	2	4	8	12
3	7	−1	12	34	46
4	12	6	30	110	140
5	20	−6	68	304	372
6	33	21	144	760	904
7	53	−31	291	1763	2054
8	85	83	566	3878	4444
9	133	−147	1069	8151	9220
10	210	346	1970	16586	18556
11	322	−678	3557	32689	36246
12	505	1521	6316	63112	69428
13	759	−3127	11040	118800	129840
14	1192	6824	19080	220888	239968
15	1748	−14364	32528	401410	433938
16	2782	31170	55086	725966	781052
17	3931	−66549	92016	1281678	1373694
18	6476	143800	153484	2272152	2425636
19	8579	−308723	251825	3909039	4160864
20	15216	667802	415704	6842392	7258096
21	17847	−1441743	670169	11469139	12139308
22	36761	3120987	1100920	19993104	21094024
23	33612	−6749982			
24	93961	14632457			

(*c*) The triangular lattice bond problem ($a = 2$)

m	$S(p)$	$S_0(p)$	$\mu_2^{(x)}$	$\mu_2^{(t)}$	$\mu_2^{(r)}$
0	1	1	0	0	0
1	3	1	6	6	12
2	9	3	36	68	104
3	25	5	162	442	604
4	66	14	618	2218	2836
5	168	26	2136	9528	11664
6	417	59	6882	36834	43716
7	1014	130	21072	131856	152928
8	2427	269	61968	445000	506968
9	5737	561	176526	1433294	1609820
10	13412	1290	489750	4444006	4933756
11	31088	2574	1329186	13349510	14678696
12	71506	5400	3540468	39041224	42581692
13	163378	12252	9278892	111583236	120862128
14	371272	25112	23979348	312618368	336597716

(*d*) The triangular lattice site problem ($a = 2$)

m	$S(p)$	$S_0(p)$	$\mu_2^{(x)}$	$\mu_2^{(t)}$	$\mu_2^{(r)}$
0	1	1	0	0	0
1	3	1	6	6	12
2	7	1	36	60	96
3	15	3	138	314	452
4	31	5	432	1240	1672
5	62	6	1206	4166	5372
6	122	14	3120	12600	15720
7	235	25	7644	35324	42968
8	448	32	17976	93576	111552
9	842	70	40896	236944	277840
10	1572	116	90660	578764	669424
11	2904	176	196458	1371478	1567936
12	5341	337	418212	3169380	3587592

References

Arrowsmith D K and Essam J W 1977 *J. Math. Phys.* **18** 235–8
Abarbanel H P, Bronzan J B, Schwimmer A and Sugar R L 1976 *Phys. Rev.* D **14** 632
Blease J 1976 *PhD Thesis* University of London
—— 1977a *J. Phys. C: Solid State Phys.* **10** 3461–76
—— 1977b *J. Phys. C: Solid State Phys.* **10** 925–36
—— 1977c *J. Phys. C:* Solid State Phys. **10** 917–24
Blease J, Essam J W and Place C M 1978 *J. Phys. C: Solid State Phys.* **11** 4009–16
Broadbent S R and Hammersley J M 1957 *Proc. Camb. Phil. Soc.* **53** 629–41
Cardy J L and Sugar R L 1980 *J. Phys. A: Math. Gen.* **13** L423–7
Coniglio A and Essam J W 1977 *J. Phys. A: Math. Gen.* **10** 1917–26
De'Bell K and Essam J W 1981 *J. Phys. A: Math. Gen.* **14** 1993–2008
Domb C 1959 *Nature* **184** 509–12

Dunn A G, Essam J W and Loveluck J M 1975a *J. Phys. C: Solid State Phys.* **8** 743–50
Dunn A G, Essam J W and Ritchie D S 1975b *J. Phys. C: Solid State Phys.* **8** 4219–35
Essam J W 1980 *Rep. Prog. Phys.* **43** 833–912
Essam J W and De'Bell K 1981 *J. Phys. A: Math. Gen.* **14** L459–61
Grassberger P 1982 *Preprint, On the Critical Behaviour of the General Epidemic Process and Dynamical Percolation*
Grassberger P and de la Torre A 1979 *Ann. Phys., NY* **122** 373–96
Harms B C and Strayley J P 1982 *J. Phys. A: Math. Gen.* **15** 1867–72
Kinzel W and Yeomans J M 1981 *J. Phys. A: Math. Gen.* **14** L163–8
Mauldon J G 1961 *Proc. 4th Berkely Symp.* **1** 337–45
Obukhov S P 1980 *Physica* **101A** 145–55
Redner S 1982a *Phys. Rev.* B **25** 3243–50
—— 1982b *Phys. Rev.* B **25** 5646–55
Redner S and Brown A C 1981 *J. Phys. A: Math. Gen.* **14** L285–90
Schögl F 1972 *Z. Phys.* **253** 147
Schulman L S 1982 *Preprint, Percolation Analysis of Stochastic Models of Galactic Evolution*
Skal A S and Skhlovskii B J 1975 *Sov. Phys.–Semicond.* **80** 1029–32